Biomedical Optics EXPRESS

Endoscopic probe optics for spectrally encoded confocal microscopy

DongKyun Kang,[1] Robert W. Carruth,[1] Minkyu Kim, [1,2] Simon C. Schlachter,[1] Milen Shishkov, [1] Kevin Woods,[1] Nima Tabatabaei, [1] Tao Wu,[1] and Guillermo J. Tearney[1,3,4,*]

[1]*Harvard Medical School and Wellman Center for Photomedicine, Massachusetts General Hospital, 55 Fruit Street, Boston, MA 02114, USA*

[2]*School of Engineering, The University of Tokyo, Yayoi 2-11-16 Bunkyo, Tokyo 113-8656, Japan*

[3]*Harvard-MIT Division of Health Sciences and Technology, 77 Massachusetts Avenue, Cambridge, MA 02139, USA*

[4]*Department of Pathology, Harvard Medical School and Massachusetts General Hospital, 55 Fruit Street, Boston, MA 02114, USA*

[*] *gtearney@partners.org*

Abstract: Spectrally encoded confocal microscopy (SECM) is a form of reflectance confocal microscopy that can achieve high imaging speeds using relatively simple probe optics. Previously, the feasibility of conducting large-area SECM imaging of the esophagus in bench top setups has been demonstrated. Challenges remain, however, in translating SECM into a clinically-useable device; the tissue imaging performance should be improved, and the probe size needs to be significantly reduced so that it can fit into luminal organs of interest. In this paper, we report the development of new SECM endoscopic probe optics that addresses these challenges. A custom water-immersion aspheric singlet (NA = 0.5) was developed and used as the objective lens. The water-immersion condition was used to reduce the spherical aberrations and specular reflection from the tissue surface, which enables cellular imaging of the tissue deep below the surface. A custom collimation lens and a small-size grating were used along with the custom aspheric singlet to reduce the probe size. A dual-clad fiber was used to provide both the single- and multi- mode detection modes. The SECM probe optics was made to be 5.85 mm in diameter and 30 mm in length, which is small enough for safe and comfortable endoscopic imaging of the gastrointestinal tract. The lateral resolution was 1.8 and 2.3 μm for the single- and multi- mode detection modes, respectively, and the axial resolution 11 and 17 μm. SECM images of the swine esophageal tissue demonstrated the capability of this device to enable the visualization of characteristic cellular structural features, including basal cell nuclei and papillae, down to the imaging depth of 260 μm. These results suggest that the new SECM endoscopic probe optics will be useful for imaging large areas of the esophagus at the cellular scale *in vivo*.

OCIS codes: (170.1790) Confocal microscopy; (170.2150) Endoscopic imaging; (170.2680) Gastrointestinal; (170.4730) Optical pathology.

References and links

1. G. J. Tearney, R. H. Webb, and B. E. Bouma, "Spectrally encoded confocal microscopy," Opt. Lett. **23**(15), 1152–1154 (1998).
2. Y. K. Tao and J. A. Izatt, "Spectrally encoded confocal scanning laser ophthalmoscopy," Opt. Lett. **35**(4), 574–576 (2010).
3. L. Golan, D. Yeheskely-Hayon, L. Minai, and D. Yelin, "High-speed interferometric spectrally encoded flow cytometry," Opt. Lett. **37**(24), 5154–5156 (2012).

#194298 - $15.00 USD Received 22 Jul 2013; revised 28 Aug 2013; accepted 28 Aug 2013; published 3 Sep 2013

4. R. Kiesslich, L. Gossner, M. Goetz, A. Dahlmann, M. Vieth, M. Stolte, A. Hoffman, M. Jung, B. Nafe, P. R. Galle, and M. F. Neurath, "In vivo histology of Barrett's esophagus and associated neoplasia by confocal laser endomicroscopy," Clin. Gastroenterol. Hepatol. **4**(8), 979–987 (2006).
5. S. Kitabatake, Y. Niwa, R. Miyahara, A. Ohashi, T. Matsuura, Y. Iguchi, Y. Shimoyama, T. Nagasaka, O. Maeda, T. Ando, N. Ohmiya, A. Itoh, Y. Hirooka, and H. Goto, "Confocal endomicroscopy for the diagnosis of gastric cancer in vivo," Endoscopy **38**(11), 1110–1114 (2006).
6. A. M. Buchner, M. W. Shahid, M. G. Heckman, M. Krishna, M. Ghabril, M. Hasan, J. E. Crook, V. Gomez, M. Raimondo, T. Woodward, H. C. Wolfsen, and M. B. Wallace, "Comparison of Probe-Based Confocal Laser Endomicroscopy With Virtual Chromoendoscopy for Classification of Colon Polyps," Gastroenterology **138**(3), 834–842 (2010).
7. V. Becker, T. Vercauteren, C. H. von Weyhern, C. Prinz, R. M. Schmid, and A. Meining, "High-resolution miniprobe-based confocal microscopy in combination with video mosaicing (with video)," Gastrointest. Endosc. **66**(5), 1001–1007 (2007).
8. D. Yelin, C. Boudoux, B. E. Bouma, and G. J. Tearney, "Large area confocal microscopy," Opt. Lett. **32**(9), 1102–1104 (2007).
9. D. Kang, H. Yoo, P. Jillella, B. E. Bouma, and G. J. Tearney, "Comprehensive volumetric confocal microscopy with adaptive focusing," Biomed. Opt. Express **2**(6), 1412–1422 (2011).
10. S. C. Schlachter, D. Kang, M. J. Gora, P. Vacas-Jacques, T. Wu, R. W. Carruth, E. J. Wilsterman, B. E. Bouma, K. Woods, and G. J. Tearney, "Spectrally encoded confocal microscopy of esophageal tissues at 100 kHz line rate," Biomed. Opt. Express **4**(9), 1636–1645 (2013).
11. C. Boudoux, "Wavelength swept spectrally encoded confocal microscopy for biological and clinical applications," (MIT, Cambridge, 2007).
12. D. Yelin, B. E. Bouma, S. H. Yun, and G. J. Tearney, "Double-clad fiber for endoscopy," Opt. Lett. **29**(20), 2408–2410 (2004).
13. B. J. Vakoc, M. Shishko, S. H. Yun, W.-Y. Oh, M. J. Suter, A. E. Desjardins, J. A. Evans, N. S. Nishioka, G. J. Tearney, and B. E. Bouma, "Comprehensive esophageal microscopy by using optical frequency-domain imaging (with video)," Gastrointest. Endosc. **65**(6), 898–905 (2007).
14. D. Kang, M. J. Suter, C. Boudoux, H. Yoo, P. S. Yachimski, W. P. Puricelli, N. S. Nishioka, M. Mino-Kenudson, G. Y. Lauwers, B. E. Bouma, and G. J. Tearney, "Comprehensive imaging of gastroesophageal biopsy samples by spectrally encoded confocal microscopy," Gastrointest. Endosc. **71**(1), 35–43 (2010).
15. DuPont, "DuPont FEP Film", retrieved *http://www2.dupont.com/Teflon_Industrial/en_US/assets/downloads/h55007.pdf*.
16. D. K. Kang, M. J. Suter, C. Boudoux, P. S. Yachimski, W. P. Puricelli, N. S. Nishioka, M. Mino-Kenudson, G. Y. Lauwers, B. E. Bouma, and G. J. Tearney, "Co-registered spectrally encoded confocal microscopy and optical frequency domain imaging system," J. Microsc. **239**(2), 87–91 (2010).
17. C. Glazowski and M. Rajadhyaksha, "Optimal detection pinhole for lowering speckle noise while maintaining adequate optical sectioning in confocal reflectance microscopes," J. Biomed. Opt. **17**(8), 085001 (2012).
18. S. Lemire-Renaud, M. Rivard, M. Strupler, D. Morneau, F. i. Verpillat, X. Daxhelet, N. Godbout, and C. Boudoux, "Double-clad fiber coupler for endoscopy," Opt. Express **18**(10), 9755–9764 (2010).
19. G. Ren, P. Shum, J. Hu, X. Yu, and Y. Gong, "Fabrication of all-solid photonic bandgap fiber coupler," Opt. Lett. **32**(21), 3059–3061 (2007).
20. M. Guelrud, I. Herrera, H. Essenfeld, and J. Castro, "Enhanced magnification endoscopy: A new technique to identify specialized intestinal metaplasia in Barrett's esophagus," Gastrointest. Endosc. **53**(6), 559–565 (2001).
21. J. L. Vázquez-Iglesias, P. Alonso-Aguirre, M. T. Diz-Lois, M. A. Vázquez-Millán, A. Alvarez, and M. J. Lorenzo, "Acetic acid allows effective selection of areas for obtaining biopsy samples in Barrett's esophagus," Eur. J. Gastroenterol. Hepatol. **19**(3), 187–193 (2007).

1. Introduction

Spectrally encoded confocal microscopy (SECM) is a form of reflectance confocal microscopy that can achieve very high imaging speeds [1]. In SECM, light with a broad spectral bandwidth is delivered by an optical fiber to the distal optics. At the distal optics, the light is first collimated and then incident on a diffraction grating. Each wavelength of the collimated light is diffracted by the grating at a unique angle and is subsequently focused by an objective lens on a distinct point on the sample. Therefore, there is a one-to-one relationship between the wavelength and transverse coordinate of the sample plane. Light reflected by the sample is coupled back to the optical fiber and then delivered to the proximal detection optics. The detection optics rapidly acquires the spectrum of the reflected light, which is also the line image of the sample. Since SECM can acquire line confocal microscopy images of the sample using only a stationary optical element, the diffraction grating, it can acquire images at a very high imaging rate [2, 3] and is well suited for being implemented in a small diameter endoscopic probe.

#194298 - $15.00 USD Received 22 Jul 2013; revised 28 Aug 2013; accepted 28 Aug 2013; published 3 Sep 2013

One promising clinical application for endoscopic SECM is large-area confocal endomicroscopy of the esophagus *in vivo*. While confocal laser endomicroscopy (CLE) has been successfully used to visualize cellular details of various gastrointestinal diseases *in vivo* [4–6], the area of the tissue that can be imaged with CLE is typically small (<0.25 mm^2). Due to its small imaging area, CLE like biopsy is prone to have sampling error by missing regions that are important for patient diagnosis. The FOV for CLE can be increased by manually moving the CLE probe and by mosaicking the CLE images [7], but the resulting FOV is still not large enough to examine the entire distal esophagus. While SECM also has a small FOV due to the use of a high-NA objective lens, the SECM FOV can be rapidly moved to image the entire distal esophagus by helically scanning the SECM optics within the probe.

We have previously developed SECM bench top scanning systems and have demonstrated the feasibility of conducting large-area SECM imaging of luminal organs [8, 9]. A side-looking SECM bench top probe mockup was demonstrated that helically scanned the SECM optics to image large areas of a cylindrical sample [8]. With this bench top system, a 2.5-cm segment of a tissue phantom (diameter = 2.0 cm) was imaged within 100 seconds. Another SECM bench top probe mockup was demonstrated that can conduct adaptive focusing. The results from this device demonstrated that a cylindrical sample with an irregular surface can be imaged over a large area [9].

While these two papers demonstrated the principles of helically scanning comprehensive confocal microscopy with SECM, they were far from being suitable for implementation in luminal organs *in vivo*. First, the optics of the bench top probe demonstrations were too large to be practical for endoscopic devices. The previous devices had a diameter of 15 mm; miniaturization by a factor of approximately 3 is required for a clinically useful probe. In addition, the tissue imaging performance for these devices was not adequate for diagnosis. In previous bench top probe setups, off-the-shelf aspheric singlets were used as the objective lenses. These aspheric singlets were designed to be used with the dry-immersion condition. Having the dry-immersion condition made the tissue imaging difficult in two different ways: 1) the spherical aberrations generated by the mismatch of refractive index between the air and tissue reduced the resolution when imaging deep inside the tissue, and (2) the specular reflection from the tissue surface overwhelmed the signal generated from the superficial region of the tissue and prevented the illumination light from reaching deep into the tissue. As a result, previous SECM probe demonstrations were limited in their capability to visualize cellular and sub-cellular features of the tissue.

In this paper, we report the development of new probe optics that are specially tailored for endoscopic SECM imaging of the esophagus. The overview of the SECM endoscopic probe optics is described first, and the details of the key design features are covered. The results from the optical performance test and tissue imaging performance test are presented.

2. Methods

2.1 SECM probe optics and system

Figure 1 shows the schematic of the SECM probe optics and system. Light from a wavelength-swept source (central wavelength = 1297 nm; bandwidth = 91 nm; output power = 80 mW; repetition rate = 100 kHz) [10] was coupled to a single-mode fiber (SMF28, Corning) and then to a circulator. The light coming out from the second arm of the circulator was collimated by a collimation lens (CL; focal length = 11 mm), and the collimated light was delivered to a beam splitter (BS). Approximately half of the collimated light was transmitted by the beam splitter and was coupled to the core of a dual clad fiber (DCF; core diameter = 7.18 μm; inner clad diameter = 29.1 μm; core NA = 0.123; inner clad NA = 0.124; length = ~2m). The specifications of the DCF were determined by the numerical and experimental analyses of the speckle contrast and axial resolution. The numerical and experimental analysis results showed that the core-to-inner clad ratio of this DCF, ~4,

#194298 - $15.00 USD Received 22 Jul 2013; revised 28 Aug 2013; accepted 28 Aug 2013; published 3 Sep 2013

significantly reduces the speckle contrast while maintaining good enough axial resolution for cellular imaging [11]. The other half of the collimated light was reflected by the beam splitter and was not used for SECM imaging.

The light coupled to the core of the DCF was delivered to the probe optics. The light coming out from the DCF was collimated by a lens and then illuminated a diffraction grating (groove density = 1144 line/mm). The diffracted light was focused into a focal line inside the tissue by a water-immersion objective lens. We specially designed and fabricated the collimation lens, diffraction grating, and objective lens to achieve good microscopic tissue imaging performance and to reduce the probe size. These optical components will be described in more detail in the following sections.

Light reflected by the tissue was delivered back to the DCF and was coupled to both the core and inner clad of the DCF. The inner clad light coupling was used to reduce the speckle noise [12]. At the proximal end of the DCF, the light returning from the probe was collimated by another collimation lens (focal length = 11 mm) and was divided by the beam splitter into two beams. Half of the light was coupled to the circulator and was used for the single-mode detection. The other half was coupled to a multi-mode fiber (MMF; core diameter = 62.5 μm) and used for the multi-mode detection. Two photo detectors were used: the first detector received the single-mode light coming from the circulator, and the second detector the multi-mode light coming from the MMF.

In the future, when performing endomicroscopic imaging within the human esophagus *in vivo*, the probe will be designed to operate similarly to other helically scanning probes that we have developed in our laboratory [13], as described below. The optical probe will be inserted into a transparent sheath (inner diameter = 5.96 mm; outer diameter = 6.93 mm). The transparent sheath will be closed at the distal end and prevents the probe from having any contact with the tissue. At the end of the SECM endoscopic imaging, the transparent sheath will be disposed, while the probe will be cleaned and re-used for the next human subject without posing any significant risk of infection. The probe will be rotated by a fiber optic rotary junction and pulled back by a translation stage to image a large area of the esophagus. Both the rotary junction and translation stage will be located outside the human subject.

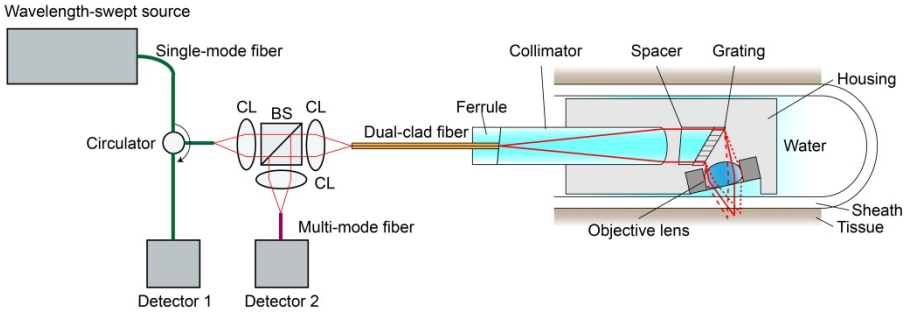

Fig. 1. Schematic of SECM probe optics and system. CL – collimation lens; and BS – beam splitter.

2.2 Rod collimation lens and small-size grating

We have developed a custom rod lens as the collimation lens in the SECM probe. The rod lens had a spherical surface at the distal end to collimate the beam. The shape of the spherical surface and the length of the rod lens were determined through iterative optimization via ZEMAX (Zemax, WA). The rod lens was made of BK7 and had a diameter of 2.0 mm, length of 16 mm, and radius of curvature of 5.44 mm. The designed rod lens generated a collimated beam with the diameter of 1.9 mm for the NA of 0.09, which was the Gaussian NA of the DCF core. The ZEMAX simulation showed that the collimated beam had the RMS wavefront error less than 0.02 over the entire source spectrum. The performance of the rod lens was

#194298 - $15.00 USD Received 22 Jul 2013; revised 28 Aug 2013; accepted 28 Aug 2013; published 3 Sep 2013

better than that of the collimation optics that we designed using the off-the-shelf GRIN lens and spacer with the same diameter. The proximal end of the rod lens was polished at 4° to reduce the back reflection. The rod lens was bonded to the DCF using a UV curing epoxy (OG172, Epoxy Technology, MA).

We have made a small-size grating (diameter = 2.2 mm) for the SECM probe. The small-size grating was made by machining an off-the-shelf fused silica grating (grating area = 14 mm by 11.5 mm; thickness = 0.625 mm). First, the off-the-shelf grating was mounted on a milling machine. Then a diamond-coated core drill bit was used to cut the small-size grating. The core drill bit was mounted at 30° relative to the normal axis of the grating surface to generate the elliptical profile for the machined grating. In the probe, the small-size grating was assembled with a 2.0-mm-diameter spacer that was polished at 30° at the distal end. Use of the spacer changed the Littrow incidence angle at the central wavelength from 47.5° (when the incidence medium is air) to 30°. As a result, the propagation angle of the diffracted beam measured relative to the normal axis of the tissue surface was also changed from −5° to 12.5°. With the 12.5° propagation angle, we were able to place the objective lens closer to the grating than with the −5° propagation angle, which reduced the probe diameter. The 12.5° propagation angle induced more tilt of the focal line, which was beneficial in increasing the range of imaging depths. More details about the range of imaging depths will be covered in the next section. Finally, the 12.5° propagation angle reduced the collection of the specular reflection more than the −5° angle.

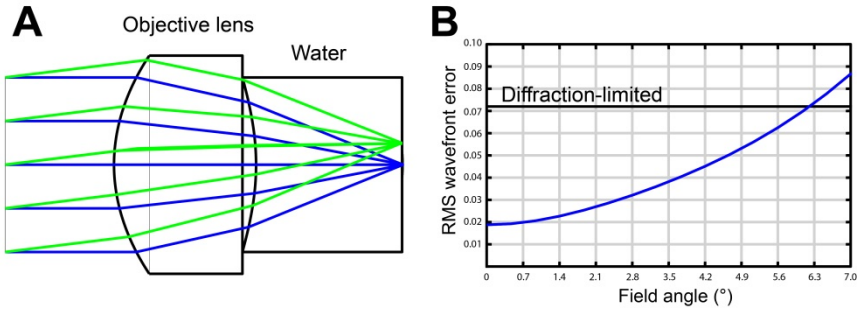

Fig. 2. ZEMAX simulation of SECM objective lens. A – layout of the objective lens with ray tracing; and B – RMS wavefront error as a function of the field angle.

2.3 Water-immersion objective lens

We developed a water-immersion aspheric singlet as the objective lens for the SECM endoscopic probe. Water was chosen as the immersion medium between the objective lens and tissue, since the water-immersion condition provides less spherical aberrations than the dry-immersion case. Also, we have chosen to use an aspheric singlet based on the following advantages. The thickness of the aspheric singlet can be made significantly smaller than that of the multi-element objective lens. The aspheric singlet can achieve fairly large NA, typically up to 0.7, while maintaining diffraction-limited performance. The aspheric singlet can be made by a compression molding process, where a glass preform is placed in a precisely machined mold and compressed into the lens shape under high temperature and pressure. The cost of the compression molding process is low, about $35 per lens, after the initial cost for fabricating the mold.

The layout of the lens is shown in Fig. 2(a). L-LAH84 (refractive index at 1290 nm = 1.78) was chosen as the lens material. Both surfaces of the lens were assigned to be aspherical. The thickness and the shapes of the two surfaces were determined using the optimization tool in ZEMAX. The designed lens had the focal length of 2.13 mm in water; working distance 1 mm; clear aperture 1.60 mm; and effective NA 0.5. Figure 2(b) shows the RMS wavefront error as a function of the field angle at the central wavelength of the source.

#194298 - $15.00 USD Received 22 Jul 2013; revised 28 Aug 2013; accepted 28 Aug 2013; published 3 Sep 2013

The lens had a diffraction-limited performance over the field angle of ± 6.2°, which corresponded to the field size of 460 μm. Anti-reflection (AR) coatings were placed on the two surfaces: the air-to-glass AR coating for the first surface; and the glass-to-water AR coating for the second surface. Both AR coatings had transmittance over 99%. A stainless steel housing (diameter = 3.0 mm; thickness = 1.4 mm) was used to protect the lens surfaces and to make it easy to assemble the objective lens with the probe housing.

In the probe, the objective lens was tilted by 12.5° relative to the normal axis of the tissue. The titled arrangement of the objective lens generated a focal line that was not parallel to the tissue surface but spanned over a range of depths as shown in Fig. 1. The titled objective configuration enabled SECM imaging at multiple depth levels during a single helical scan [9]. With the given spectrum of the source and groove density of the grating, the width of the focal line was 255 μm. The focal line was centered at 100 μm below the tissue surface and extended over 54 μm. The 100 μm imaging depth was chosen because our previous study of imaging human esophageal tissues with SECM showed that the SECM images taken from the imaging depth between 50 and 150 μm can visualize key histomorphologic information associated with various epithelial diseases [14].

In order to maintain uniform refractive index between the objective lens and tissue, we made a careful selection of the sheath material and filled the space between the sheath and objective lens with water. Fluorinated ethylene polymer (FEP) was used as the sheath material, since its refractive index, 1.34, is very close to that of water. FEP also has other merits as the sheath material: it has high transmittance (over 90%) for the spectrum of the source; and it has low friction coefficient (0.25), which can facilitate the smooth scan of the probe inside the sheath [15].

2.4 Performance test

The lateral resolution was tested by imaging a USAF resolution target and by measuring the FWHM of the line-spread function (LSF). The axial resolution was measured by obtaining multiple images of a mirror while axially scanning the mirror. An intensity curve was generated from the axial scan, and the FWHM of the intensity curve was calculated as the axial resolution. The resolutions were measured for both the single-mode and multi-mode detection modes.

The field of view (FOV) was measured by imaging a Ronchi ruling glass slide (frequency = 400 lines/mm). The range of imaging depths was measured by obtaining three-dimensional image stack of a mirror while axially scanning the mirror. The three-dimensional image stack was resampled along the axial direction to produce cross-sectional images, which showed the mirror as a tilted line that spanned over a range of depths. From the cross-sectional image, the depth difference between the two focal points at the edges of the FOV was calculated as the range of the imaging depths.

Tissue imaging performance was tested by imaging excised swine esophageal tissue. The swine tissue was treated with 6% acetic acid prior to the SECM imaging to increase the nuclear contrast. A thin FEP sheet (thickness = 250 μm) was placed on the tissue to simulate the use of the FEP sheath during *in vivo* endoscopic imaging. Water immersion was used between the objective lens and FEP sheet. The swine tissue was scanned using a two-axis translation stage to obtain large-area SECM images. Multiple depths of the tissue were imaged by translating the probe axially with a single-axis translation stage.

#194298 - $15.00 USD Received 22 Jul 2013; revised 28 Aug 2013; accepted 28 Aug 2013; published 3 Sep 2013

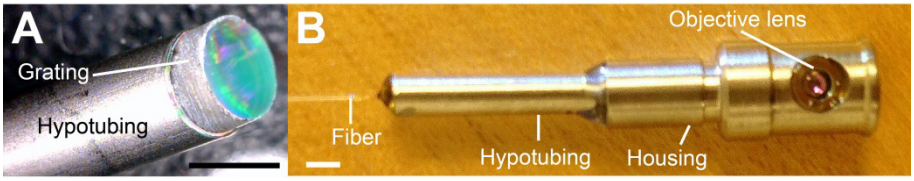

Fig. 3. Photographs of SECM endoscopic probe. A – collimation optics; and B – final probe assembly. Scale bar = 2 mm.

3. Results

3.1 Probe fabrication

A photograph of the collimation optics is shown in Fig. 3(a). The ferrule, collimation lens, and spacer were housed inside a hypotubing, which provided mechanical integrity of the collimation optics. The grating was placed at the tip of the hypotubing. As shown in Fig. 3(a), the miniature grating had a clear aperture that had almost the same diameter as the physical diameter of the grating. For most of the cases, the machined grating had a clear aperture that was larger than 90% of the physical diameter. A photo of the assembled probe is shown in Fig. 3(b). The probe had an outer diameter of 5.85 mm and a length of 30 mm. The probe was completely sealed to water, and the optical performance of the probe did not degrade after multiple water-immersion imaging sessions. Back-reflection from the probe optics was measured to be −55 dB.

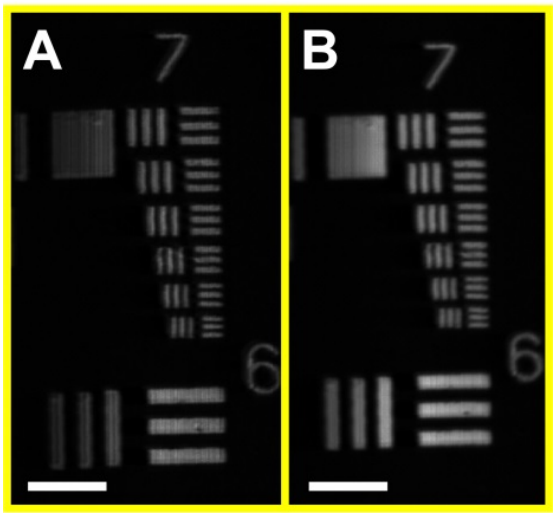

Fig. 4. SECM images of USAF resolution target. A – single-mode detection; and B- multi-mode detection. Scale bars = 50 µm.

3.2 Resolution and FOV

Figure 4 shows SECM images of the USAF resolution target using the single-mode and multi-mode detection methods. Both the single- and multi- mode detection methods were able to clearly visualize the smallest pattern at group 7, element 6. The FWHM's of the LSF's were measured as 1.8 and 2.3 µm for the single- and multi- mode detection methods, respectively. Figure 5 shows the axial response curves for the single- and multi- mode detection methods. The axial response curve for the single-mode detection (black curve) had a narrower main lobe than the curve for the multi-mode detection (red curve). The FWHM's of the axial response curves were measured as 11 and 17 µm for the single- and multi- mode

#194298 - $15.00 USD Received 22 Jul 2013; revised 28 Aug 2013; accepted 28 Aug 2013; published 3 Sep 2013

detection methods, respectively. FOV was measured to be 280 μm, and the range of imaging depths was measured to be 57 μm.

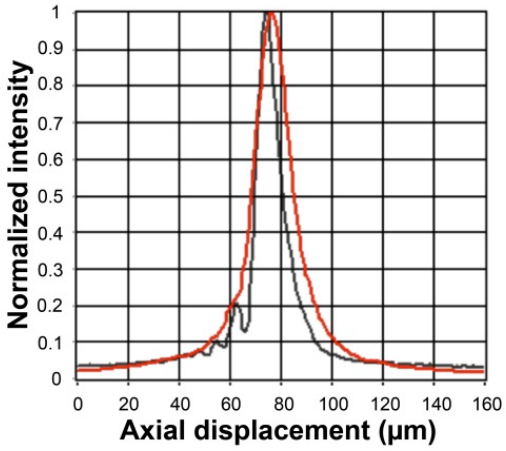

Fig. 5. Axial response curves for the single-mode (black) and multi-mode (red) detection methods.

3.3 Tissue imaging

Figure 6 shows SECM images of the swine esophageal tissue taken with the single-mode (Fig. 6(a), 6(c), and 6(e)) and multi-mode (Fig. 6(b), 6(d), and 6(f)) detection methods. Images were taken at the same transverse location and at multiple imaging depths. Images taken at a depth of 130 μm (Fig. 6(a) and 6(b) enable clear visualization of basal cell nuclei (circles). Images taken at the depth of 160 μm (Fig. 6(c) and 6(d)) begin to reveal esophageal squamous papillae (arrows). Images taken at the depth of 260 μm (Fig. 6(e) and 6(f)) show bases of papillae (arrows).

Differences between the single- and multi- mode detections were observed. The signal detected by the single-mode detection was smaller than that detected by the multi-mode detection by approximately a factor of five. Due to the small signal level, the single-mode image at the imaging depth of 260 μm (Fig. 6(e)) had poorer signal-to-noise ratio (SNR) than that of the multi-mode image (Fig. 6(f)). Difference in the speckle noise contrast was observed in higher-magnification images (Fig. 7). While the single-mode image (Fig. 7(a)) had apparent speckle noises with a contrast of 1, the multi-mode image (Fig. 7(b)) had less speckle noise with a contrast of 0.4.

4. Discussion

In this paper, we have reported the development of new SECM endoscopic probe optics. In the new probe optics, custom miniature optical components were designed and fabricated to reduce the probe size and to achieve good tissue imaging performance. The SECM probe optics was 5.85 mm in diameter, which is sufficiently small to be safe and comfortable for imaging the esophagus, considering the diameter of a typical video endoscope is larger than 10 mm. The SECM probe optics were able to visualize characteristic cellular features of the swine esophageal tissue down to an imaging depth of 260 μm. These results suggest that the SECM probe optics will be capable of successfully imaging large areas of the esophagus *in vivo*.

#194298 - $15.00 USD Received 22 Jul 2013; revised 28 Aug 2013; accepted 28 Aug 2013; published 3 Sep 2013

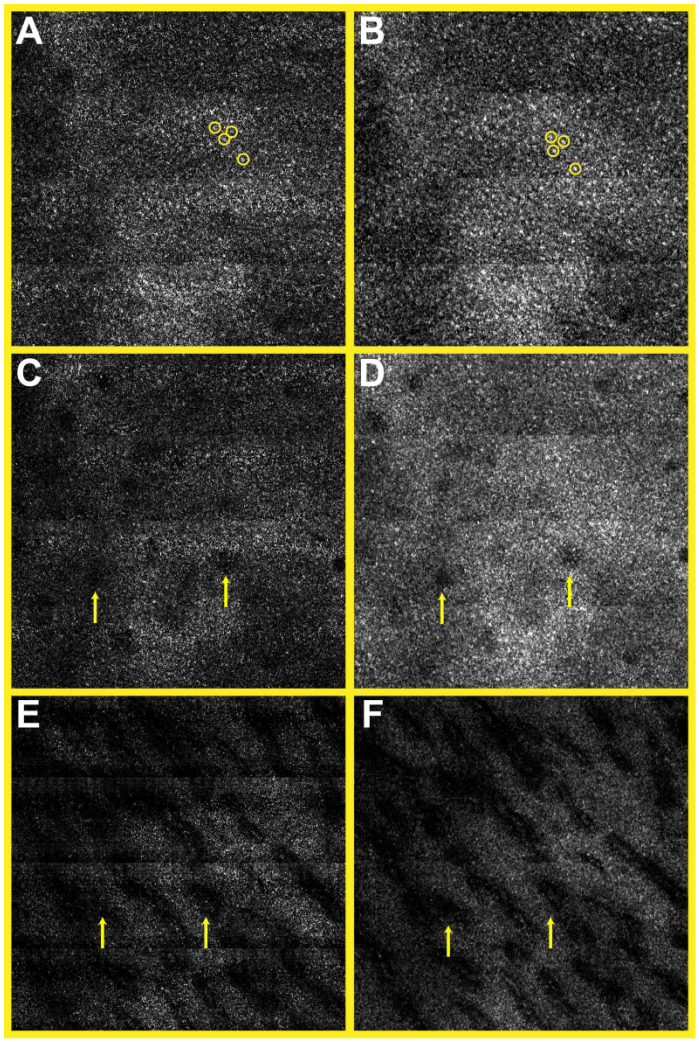

Fig. 6. SECM images of swine esophageal tissue *ex vivo* taken from the imaging depths of 130 µm (A, B), 160 µm (C, D), and 260 µm (E,F). A, C, E – single-mode images; and B, D, F – multi-mode images. circles – basal cell nuclei; and arrows – papillae. Size of each image = 700 µm × 700 µm.

#194298 - $15.00 USD Received 22 Jul 2013; revised 28 Aug 2013; accepted 28 Aug 2013; published 3 Sep 2013

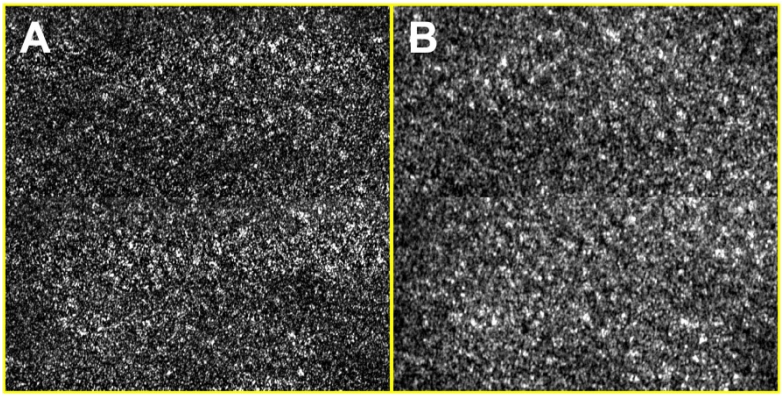

Fig. 7. High-magnification SECM images of swine esophageal tissue *ex vivo*. A – single-mode image; and B – multi-mode image. Size of each image = 350 μm × 350 μm.

We did find areas where we can further improve the performance of the probe optics. The axial resolution of the probe optics (17 μm for the multi-mode detection) was worse than the axial resolution of the SECM bench top optics (10 μm for the multi-mode detection) [14]. The difference in the axial resolution was mainly caused by the difference in the objective lens NA: 0.5 for the probe optics and 0.7 for the bench top optics. The tissue imaging results in this paper showed that the probe optics, with the 17-μm axial resolution, can clearly visualize cellular features of the swine esophagus. We, therefore, expect the probe optics will be able to visualize key cellular features of the human esophagus during the *in vivo* human imaging. However, if we find that better resolution is needed, we will design a new custom aspheric singlet that has higher NA. There are several off-the-shelf aspheric singlets that have NA's higher than 0.7. We expect that we will be able to design a water-immersion aspheric singlet that has NA of 0.7 or higher. The high NA lens, however, is likely to have a shorter focal length and a smaller FOV, which may increase the imaging time noticeably when imaging a large mucosal area.

The axial response curve for the single-mode detection had noticeable side lobes. The side lobes were probably caused by the fabrication errors in the objective lens and by the alignment errors between the optical components. In the axial response curve, the area under the first side lobe, located 10 μm away from the main lobe, was approximately 10% of the area under the main lobe. This implies that the light reflected from the first side lobe contributed 10 times less to the detected signal than the light reflected from the main lobe did. The single-mode images of the swine esophagus showed that the signal from the nucleus was 2 to 3 times stronger than that from the non-nuclear tissue elements. Therefore, it is unlikely that the side lobes affected the nuclear contrast significantly. The side lobes can be reduced by tightening tolerances on the objective lens fabrication and/or by constructing an alignment setup with higher precision. This remedy, however, is likely to increase the fabrication cost.

#194298 - $15.00 USD Received 22 Jul 2013; revised 28 Aug 2013; accepted 28 Aug 2013; published 3 Sep 2013

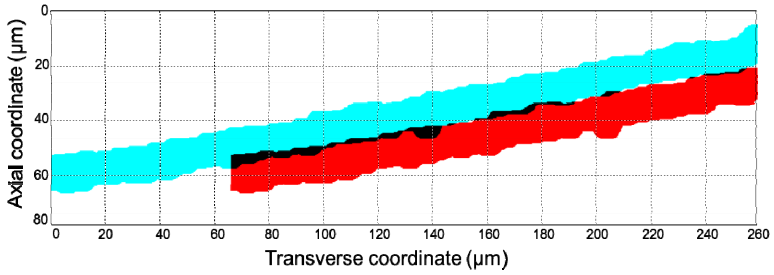

Fig. 8. SECM focal lines in the tissue space. The red line is shifted by 67 μm transversely from the blue line. Black areas show the overwrapping between the two focal lines.

The aspheric singlet approach had limited performance in reducing the chromatic aberration and Petzval field curvature. Due to the longitudinal chromatic aberration and field curvature, the illumination beam was focused into a curved line rather than a straight line. From the same data set that was used for analyzing the imaging depth range, we obtained the profile of the focal line in the tissue space. Shown in Fig. 8 is the plot of the measured focal line (blue line) with a line width of 11 μm, the axial resolution for the single-mode detection. In the procedure of obtaining volumetric data [9], the SECM probe can be moved by 67 μm transversely to generate a shifted focal line (red line). While the bottom of the first focal line coincides with the top of the second focal line on the right side of the field, the two focal lines overwraps slightly (black area) on the left side of the field. Using the same image processing method as described in our previous work [9], we can obtain images from approximately four different depth levels (= 280 μm / 67 μm). Due to the field curvature, the four imaging depth levels are not spaced uniformly. The depth difference between two neighboring imaging depth levels varies from 10 μm at the top to 13 μm at the bottom. The small amount of variation in the spacing, up to 3 μm, is not likely to affect the qualitative image analysis that we usually conduct with the SECM images.

The speckle noise contrast of the multi-mode image, 0.4, was higher than the speckle noise contrast we previously had for the SECM bench top optics, 0.25 [16]. From our previous study of imaging esophageal tissues with the SECM bench top optics, we found that the SECM images with this speckle noise contrast, 0.25, appear natural and are easy to interpret. Others also found that reflectance confocal microscopy images with this speckle noise contrast are easy to read [17]. As shown in the results in this paper, the key cellular features of the swine esophageal tissue were easily identifiable with the speckle noise contrast of 0.4. There, however, might be a need to reduce the speckle noise contrast when imaging human esophageal tissues, closer to what is considered as the ideal value, 0.25. In order to achieve this lower speckle contrast value, we can increase the diameter of the DCF inner clading to reduce the speckle noise contrast. Increasing the inner clad diameter, however, has the tradeoff that it will worsen the axial resolution [17]. Therefore, the increase of the inner cladding diameter should be accompanied with an increase of the objective lens' NA to maintain optimal axial resolution.

Half of the illumination light was reflected at the beam splitter in the DCF coupling optics and was not used for SECM imaging. A fiber-based DCF coupler has been previously demonstrated for the DCF with the 105-μm-diameter inner clad [18]. With the fiber-based coupler, most of the illumination light can be delivered to the core of the DCF without significant loss, which can increase the signal level and subsequently increase the SNR of the image. The DCF we used in this paper had an inner cladding diameter of 29.1 μm, and the relatively small inner cladding diameter might make it difficult to develop a fiber-based DCF coupler. We will take various approaches to develop a fiber-based DCF coupler that works with our DCF, including the fusing and tapering approach [18] and the side-polishing approach [19].

#194298 - $15.00 USD Received 22 Jul 2013; revised 28 Aug 2013; accepted 28 Aug 2013; published 3 Sep 2013

During the swine tissue imaging *ex vivo*, 6% concentration acetic acid was used. This is higher than the concentration that has been used for *in vivo* chromoendoscopy of the human esophagus, 1.5-3% [20, 21]. We used 6% concentration because the swine esophageal tissue images with this concentration showed a similar enhancement of nuclear contrast to the human esophageal tissue images with 0.6% concentration. The difference in the concentration might be due to the permeability difference between the swine and human esophageal tissues. In our previous study of imaging human esophageal tissues [9], we have shown that an acetic acid concentration of 0.6% can visualize key nuclear features associated with various esophageal diseases. Thus, we expect that a concentration of 0.6-3%, as typically used in the clinical setting, will be sufficient for the visualization of nuclear details of the human esophagus *in vivo*.

As a next step, we will develop the mechanical parts that are needed to helically scan the SECM probe at a uniform speed, including the torque delivery mechanism and fiber optic rotary junction. Upon the completion of the mechanical components, we will conduct animal studies where we will deliver the SECM endoscopic probe to the esophagus of a living swine and will image large areas of the swine esophagus *in vivo*. In subsequent clinical studies, we will perform large-area SECM imaging of human subjects *in vivo* for the comprehensive diagnosis of esophageal disease. We believe that the large area capabilities of this SECM probe will minimize sampling error and will therefore allow patients to receive a more accurate diagnosis than that provided by the current standard of care.

Acknowledgments

This research was supported by a sponsored research agreement with Nine Point Medical, Cambridge, MA. Dr. Schlachter is currently with Nine Point Medical. Dr. Woods is currently with Emory University Hospital, Atlanta, GA. Dr. Tearney receives sponsored research from Nine Point Medical. Drs. Shishkov and Tearney consult for Nine Point Medical. Massachusetts General Hospital has a licensing arrangement with Ninepoint Medical. Drs. Kang, Carruth, Schlachter, Shishkov, and Tearney have the rights to receive royalty payments as part of this licensing arrangement.